ORIGINAL PAPER

Dynamics of endogenous Hsp70 synthesis in the brain of olfactory bulbectomized mice

**Natalia Bobkova · Irina Guzhova · Boris Margulis ·
Inna Nesterova · Natalia Medvedinskaya ·
Alexander Samokhin · Irina Alexandrova ·
David Garbuz · Evgeny Nudler · Michael Evgen'ev**

Abstract Numerous epidemiological studies have established acute brain injury as one of the major risk factors for the Alzheimer's disease (AD). However, the lack of animal models of AD-like degeneration triggered by a defined injury hampered the development of adequate therapies. Here we report that the surgical damage of the olfactory bulbs triggers the development of several pathologies, including amyloid-β accumulation and strong decrease of neuron density in the cortex and hippocampus as well as significant disturbance of spatial memory. Characteristically, these harmful consequences of the olfactory bulbectomy (OBX) have a peculiar dynamics in time with maximal manifestation in periods of 1–1.5 months and 8 months after the surgery and, hence, exhibit biphasic pattern with almost complete recovery period taking place at 5–6 months after the operation. The quantitative determination of endogenous inducible form of Hsp70 in different brain areas of OBX mice demonstrated characteristic fluctuations of Hsp70 levels depending on the time after the operation and age of mice. Interestingly, maximal induction of Hsp70 synthesis in the hippocampus exhibits clear-cut coincidence with the recovery period in OBX animals. The observed correlation enables to suggest curing effect of Hsp70 synthesis at an earlier period of pathology development and establishes it as a possible therapeutic agent for secondary grave consequences of brain injury, such as AD-like degeneration, for which neuroprotective therapy is urgently needed.

Keywords Olfactory bulbectomy · Spatial memory · Neurodegeneration · Hsp70 · Amyloid-β (Aβ) · Alzheimer's disease

N. Bobkova · I. Nesterova · N. Medvedinskaya · A. Samokhin ·
I. Alexandrova · M. Evgen'ev
Institute of Cell Biophysics, RAS,
Pushchino, Moscow Region 142290, Russia

I. Guzhova · B. Margulis
Institute of Cytology, RAS,
St. Petersburg 194064, Russia

D. Garbuz · M. Evgen'ev (✉)
Engelhardt Institute of Molecular Biology, Russian Academy of Sciences,
Vavilov str. 32,
Moscow 119991, Russia
e-mail: misha672011@yahoo.com

E. Nudler
Department of Biochemistry, New York University School of Medicine,
New York, NY 10016, USA

Introduction

Acute neurological event, such as traumatic brain injury (TBI) and stroke, often promote further brain deterioration by initiating a cytotoxic cascade (Hemphill et al. 2011). This secondary brain injury (SBI) includes multiple long-lasting neurological impairments following TBI (Wang and Ma 2010) and has many common features with Alzheimer's disease (AD). These features include severe cognitive impairment, decrease of synaptic density, enhanced concentration of soluble Aβ oligomers, and apoptosis of neurons in specific brain areas (Johnson et al. 2010; Reisberg and Saeed 2004). SBI, which increases the risk of AD four times, may be one of the causes of sporadic AD in aging humans (Ikonomovic et al. 2004). Therefore, prevention of

SBI has a fundamental importance for prophylactics of AD development.

Endogenous heat shock proteins (Hsps) exert neuroprotective activity in rodent models of Huntington's disease, Amyotrophic Lateral Sclerosis, and other cases of neuropathologies (Cummings et al. 2001; Franklin et al. 2005; Wacker et al. 2009; Gifondorwa et al. 2007). In a cellular model of AD, Hsp70 overexpression effectively protected neurons from accumulation of Aβ (Magrané et al. 2004; Hoshino et al. 2011). Therefore, in recent decade, Hsps and in particular, Hsp70 have emerged as critical regulators of proteins associated with neurodegenerative disease pathologies including the accumulation of Aβ peptides in the brains of AD individuals (reviewed by Margulis et al. 2006; Magrane and Querfurth 2010; Calderwood 2010).

To further investigate the potential curing effect of Hsps in development of SBI, we used mice with TBI, induced by surgical removal of the olfactory bulbs. These animals, routinely used as a model of endogenous depression (Doty 2009; Wesson et al. 2010), share many abnormalities with SBI and AD, including severe memory loss (Song and Leonard 2005; Bobkova et al. 2005, 2008; Nakajima et al. 2007; Doty 2009); increased level of brain amyloid precursor protein and amyloid-β (Struble et al. 1998; Kaminina et al. 2010); massive death of neurons in the hippocampus and temporal cortex (Chételat et al. 2005; Nesterova et al. 2008; Holland et al. 2009); and deficit of serotonin, acetylcholine, and glutamatergic brain systems (Nesterova et al. 1997; Hozumi et al. 2003; Moriguchi et al. 2006). Furthermore, in OBX guinea pigs having primary amino acid structure of amyloid-β identical to the human protein, we have observed not only increased intracellular accumulation of amyloid-β in neurons of the cortex but also the formation of extracellular amyloid plaques similar to those of AD patients (Bobkova et al. 2005).

Here, we present the results of a complex analysis of various pathological consequences of olfactory bulbectomy (OBX) in mice and the results of endogenous Hsp70 level measurements in the brains of OBX- and sham-operated (SO) mice that served as controls in different postoperation time periods. We demonstrate clear-cut coincidence in time between high level of inducible Hsp70 synthesis and recovery in terms of spatial memory in OBX mice at certain stages of pathology development. The induction of Hsp70 synthesis in the brain of OBX mice observed after the operation possibly provisionally protects neurons of the hippocampus and cortex from degeneration and delays the increase of amyloid-β concentration and massive neuron death which eventually takes place in experimental animals.

Materials and methods

Animals

Adult NMRI mice (males) aged 10 weeks were maintained in their home cages in a climate-controlled room at 21–23 °C with a 12:12 h light–dark cycle and had free access to water and food. All animal experiments were performed in accordance with the guidance of the National Institutes of Health for care and use of laboratory animals, NIH Publications No. 8023, revised 1978.

Generation of OBX mice

A single burr hole (2 mm diameter) was drilled over the olfactory bulbs (2 mm anterior to the bregma, 0 mm laterally from the midline) in the scalp of mice, narcotized with Nembutal (40 mg/kg) and 0.5 % Novocaine (subcutaneous injection) for local anesthesia of the skin above skull. Both olfactory bulbs were aspirated through a blunt needle attached to a water pump. The extent of the lesion was assessed both visually and histologically after the behavioral study. SO mice routinely used as controls were treated similarly, except that the olfactory bulbs were not removed.

Detection of endogenous Hsp70 and Aβ in the mouse brain

ELISA was used to measure the levels of endogenous inducible Hsp70 and Aβ (1–40) in the brain extracts, followed brain perfusion with saline (Evans et al. 2006; Toyn et al. 2010). Briefly, ELISA measurement of Hsp70 concentration has been performed in the supernatant fraction of tissue extracts of the olfactory bulbs, hippocampus, temporal and entorhinal cortices in a solution containing 20 mM NaCl; 20 mM Tris–HCl, pH7.5; 0.1 mM EDTA; 1 % protease inhibitor cocktail. The analysis developed by the authors (B.A.M., I.G.) is based on the high affinity of Hsp70 to immobilized ATP. We perform the analysis by applying brain extracts in wells of a 96-well ELISA microplate (Greiner, Microlon, Germany) covered with ATP-ovalbumin reagent for subsequent measurement of inducible member of Hsp70 as described elsewhere (Kustanova et al. 2006).

Aβ levels were determined by solid phase sandwich ELISA (Invitrogen, Camarillo, CA) in mixed brain extract (neocortex+hippocampus) in ice cold 2 % CHAPS, 20 mM tris pH 7.7, in presence of protease inhibitors (10 μg/ml leupeptin, 10 μg/ml aprotinin, and 10 μg/ml AEBSF). A monoclonal antibody specific for N terminus of mouse Aβ was precoated onto wells of the provided microtiter strips. Samples and standard diluted in the standard buffer were incubated for 2 h at room temperature allowing the Aβ to bind the capture antibody, followed by extensive washing.

Samples were incubated with detection rabbit antibody specific for the C terminus of the Aβ (1–40) for 1 h at room temperature. After being followed by washing, samples were incubated with HRP anti-rabbit antibody for 30 min at room temperature. After removal of excess anti-rabbit antibodies, a substrate solution is added, which is acted upon by the bound enzyme to produce color.

Aβ levels were independently determined by immunological DOT analysis, and as described before (Bobkova et al. 2008; Kaminina et al. 2010), 150–200 mg of the brain tissue (the cortex and hippocampus) from the OBX and SO animals were homogenized in 0.5 ml of 70 % formic acid, maintained for 1 h, centrifuged at $100,000\,g$ for 40 min and then the supernatant fluid was evaporated on a rotor evaporator to the minimum volume, supplemented with 1 ml of twice distilled water, and the solution was neutralized to pH 7.4 with NaOH and lyophilized. We used monoclonal antibodies 4 G8 (Vector Laboratories, Burlingame, CA, USA), reacting with (17–24) amino acid sequence of Aβ in human and mouse. We also used biotinylated horse antibodies to mouse IgG (Vector Laboratories, Burlingame, CA, USA) and monoclonal antibodies to biotin (the clone BN34) conjugated with peroxidase (Sigma USA). The levels of Aβ species are presented as nanogram or picomole of Aβ per gram of wet brain, taking into account dilution factors introduced by multiple steps throughout the assay (brain homogenization and extraction procedures).

Morris water maze tests

A circular swimming tank 80 cm in diameter with a wall height of 40 cm and a hidden platform of 5 cm in diameter (State Institute of Biological Instrumentation, RAS, Russia) was filled to a depth of 30 cm with water at 23 °C and rendered opaque by the addition of powdered milk. The tank was operationally (mentally) divided into four sectors: platform target sector (third) and three other indifferent sectors Klapdor & Van der Staay (1996). The hidden platform was located in the middle of the third target sector during training trials. It was submerged at a depth of 0.5 cm so as to be invisible to a swimming animal. A video monitoring system (TSI, Germany) was used to record the major behavioral parameters in the water maze paradigm. Experiments were performed in a test room with extramaze cues to facilitate spatial learning.

Initially, all groups of OBX and SO animals were assessed in the water maze without save platform to identify any inherent sector preference. None of them showed any preference. To verify that bulbectomy per se did not induce motor or visual impairments that can affect the results of memory tests, the latencies required for all SO and OBX animals to reach the visible platform were determined (in three trials) at each investigated period after the operation. Then mice were exposed to a total of 20 training trials for

5 days. The latency period to locate the hidden platform was evaluated. Spatial memory was tested on the following day after completion of training in a single probe trial (60 s) in the absence of the hidden platform, beginning from a random position. During the probe trial, occupancy time spent in each sector was recorded. To study the dynamic of spatial memory changes, Morris water maze training trials and probe tests were carried out at 0.5, 1, 1.5, 3, 6, 8, 12, and 16 months after bulbectomy in eight groups of OBX and eight groups of SO animals, $n = 7–13$ animals per group.

Histology and morphology

General histological methods were done as described (Nesterova et al. 2008). In brief, after probe test, mice were anaesthetized by an overdose of Nembutal (60 μg/kg, i/p) and their brains were perfused with 0.1 M PBS (pH 7.4). One hemisphere was frozen on dry ice and the other was fixed in 4 % phosphate-buffered paraformaldehyde at 4 °C for 48 h before storage in 30 % sucrose. After that, 20 μm sections of the hemibrains were cut in the coronal plane on a cryostat. To study the quantity and morphological state of neurons in the temporal cortex and areas of hippocampus, sections were stained for the Nissl substance and comparative studies of the cellular composition (1,000 cells for the each structure in the each mouse) were performed. We distinguished the following categories of neuronal abnormalities: cytolysis, karyolysis, pyknosis, and vacuolization, and estimated their frequencies in relation to the quantity of the normal neurons. Data are given as mean ± SEM. Comparison between the groups were performed separately for the temporal cortex and both areas of the hippocampus (CA1 and CA3) with two-tail Student's t test. The morphometric analysis of cell density was determined in 1 mm^2 in different brain structures of OBX and SO mice using standard object micrometer. Density measurements were performed in ten microscopic views and results are presented as mean ± SEM. The data were statistically treated using Statistica 6 program. Comparisons were performed using a two-tailed Student's t test. The differences (M ± SD) were considered to be significant at $p < 0.05$.

Statistical analysis

All results are reported as means ± SEM. Significant differences between mean scores during training trials in the Morris water maze were assessed with two-way repeated measures ANOVA (Statistica 06) with Tukey's post-hoc analysis for multiple comparisons using group and trial day block number during training as sources of variation. Statistical analysis of the results of probe tests was carried out with ANOVA using group and sector of maze as sources of variation. The preference for platform target quadrant in

comparison with each indifferent quadrant was assessed by post-hoc analysis using a multiple-range LSD test. The differences between experimental groups detected by DOT and ELISA analyses were treated using a two-tailed Student's *t* test.

Results

Neuron death is increased and morphology of neurons is severely disturbed in OBX mice

The investigation of the neuronal morphology has been performed in the different brain areas in the OBX and SO groups of mice. We have focused our analysis on the cell composition of the hippocampal regions (CA1 and CA3 areas) and the temporal cortex (Fig. 1a). These brain areas play the key role in learning and memory and severely suffer in patients with AD. Results of quantitative analysis of morphological data are presented in Table 1.

The SO group did not demonstrate any significant changes in form, size, and structural organization of the neurons. On the other hand, in OBX animals, heavy pathological changes were revealed in the majority of the neurons such as pyknosis, karyolysis, cytolysis, and vacuolization (Fig. 1a). The percentage of normal cells was significantly decreased in the OBX group (Table 1). Specifically, the reduction of cell size, hyperchromatosis of the cytoplasm, pyknotic degradation, and
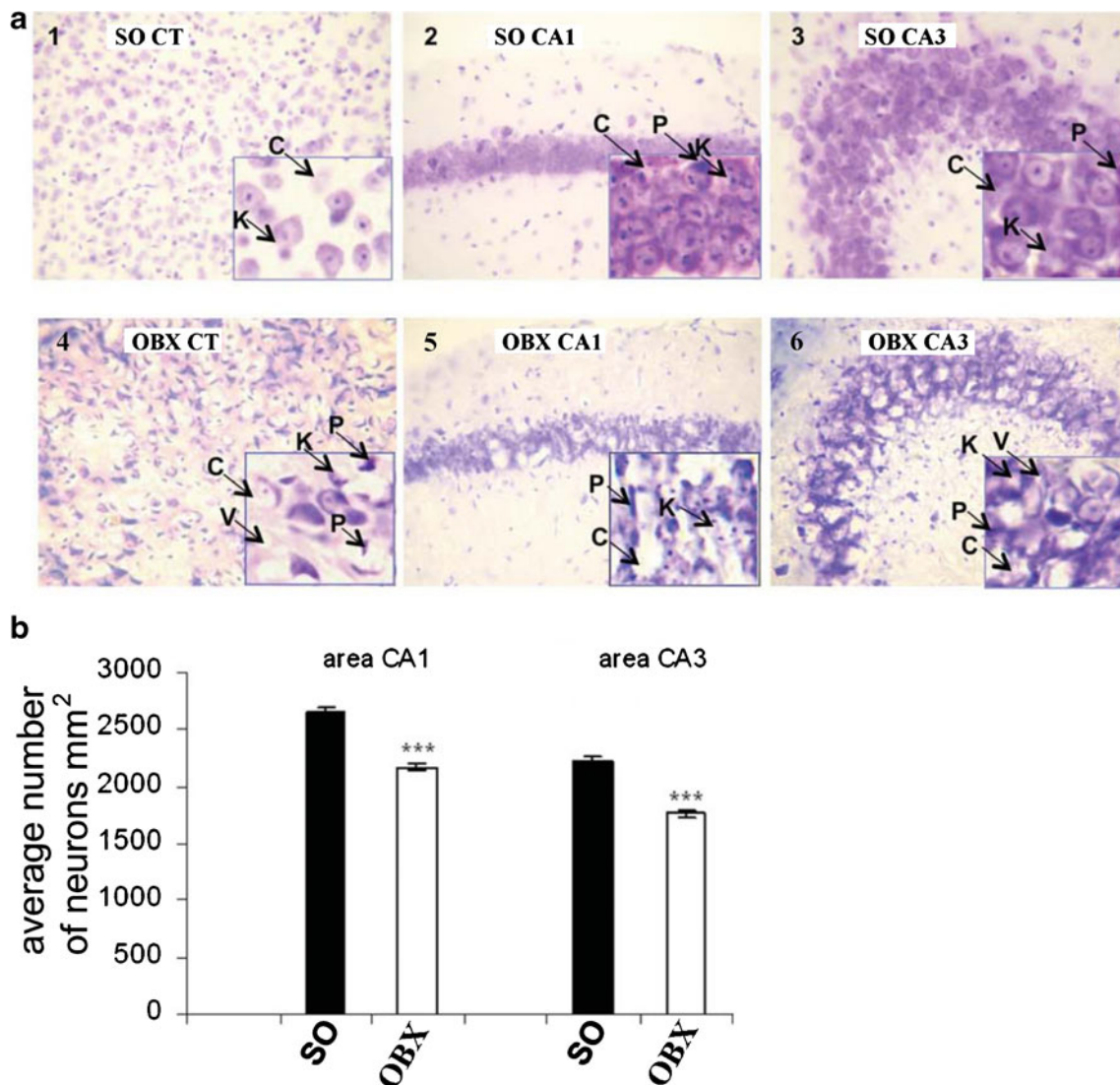

Fig. 1 Neuron morphology and density in SO and OBX mice. (**a**) Representative photomicrographs of frontal sections through the hippocampus and temporal cortices of untreated control SO mice (*1, 2, 3*) and OBX mice (*4, 5, 6*). *CT* temporal cortex, *CA1 and CA3* areas of hippocampus. Different pathological states of neurons such as pyknosis (*P*), karyolysis (*K*), cytolysis (*C*), or vacuolization (*V*) are indicated by *arrows*. (**b**) Neuronal density in CA1 and CA3 areas of hippocampus. *SO* sham-operated, *OBE* bulbectomized mice. Measurements performed 1.5 month after the surgery. *Asterisks* indicate significant differences ***$p<0.001$ relative to the SO group. **a** (×20 and ×40)

Table 1 Neuron morphology of the temporal cortex and areas of the hippocampus in SO and OBX mice

Brain areas	Groups	Kinds of neuronal pathology (%)				Normal neurons (%)
		Pyknosis	Karyolysis	Cytolysis	Vacuolization	
Temporal cortex	SO	9.9±0.68	3.1±0.23	5.9±0.49	2.7±0.38	75.9±1.1
	OBX	18.5[***]±0.66	5.7[***]±0.26	18.6[***]±0.51	2.9±0.28	53.6[***]±1.0
Hippocampus area CA1	SO	6.3±0.66	2.9±0.26	5.9±0.46	2.2±0.26	82.6±1.08
	OBX	15.9[***]±0.69	5.4[***]±0.31	17.1[***]±0.61	2.7±0.24	59.0[***]±0.87
Hippocampus area CA3	SO	4.6±0.43	2.5±0.23	5.9±0.4	1.2±0.16	85.8±0.89
	OBX	16.7[***]±0.63	5.2[***]±0.33	21.1[***]±0.58	2.6[***]±0.2	54.0[***]±0.74

Data are given as mean ± SEM. Comparison between the groups were performed separately for the temporal cortex and both areas of the hippocampus with two-tail Student's t test to compare replicate means with special emphasis on bulbectomy-induced changes

[**] $p<0.01$; [***] $p<0.001$

cytolysis represented prominent features often observed in the CA3 and CA1 areas (Fig. 1a).

Importantly, the total neuron density in CA1 and CA3 areas of the hippocampus decreased significantly ($p<0.001$) in the OBX mice in comparison with SO group (Fig. 1b). By contrast, the percentage of pyknomorphic cells in various brain structures of OBX mice dramatically increases in comparison with SO animals (Fig. 2).

Intensive accumulation of amyloid-β is observed in the brains of OBX mice

Since an abnormally high accumulation of amyloid-β peptides in afflicted regions of the brain is a biochemical hallmark of AD and has been also demonstrated in OBX mice (Reisberg and Saeed 2004; Kaminina et al. 2010), we decided to monitor the age-dependent fluctuations of Aβ peptide levels in SO and OBX mice. To estimate the kinetics of amyloid-β accumulation at different time intervals after the operation, we measured the level of amyloid-β in the pooled extracts of the cortex and hippocampus by DOT analysis using the 4 G8 monoclonal antibodies against mouse and human
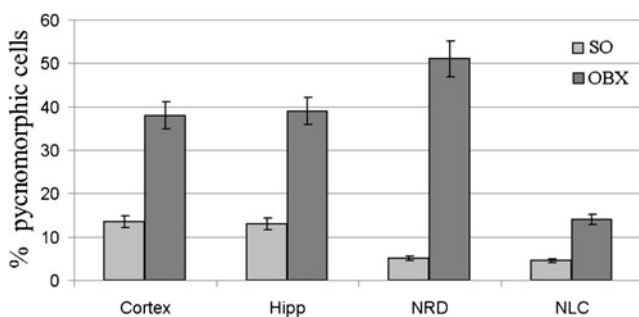
Aβ peptides and ELISA method as described in "Materials and methods". The results of representative DOT analysis are depicted in Fig. 3. Statistical analysis of the data accumulated by the two independent complementary methods clearly demonstrated dramatic increase in Aβ levels after bulbectomy (Fig. 4a and b). Importantly, both independent methods of amyloid-β measurement in SO and OBX mice produce very similar results (Fig. 4a and b).

Furthermore, DOT analysis enabled us to conclude that while the total amount of Aβ in SO and OBX groups significantly increases with age, in the OBX group, the level of Aβ was significantly higher than that in control SO ($p<0.001$) at all points of measurement (Fig. 5).

The analysis summarized described above demonstrated that brains of OBX mice exhibit various pathologies in common with AD and a few other neurodegenerative diseases. At the next stage, we decided to monitor behavior of OBX animals at different periods after the olfactory bulb ablation.
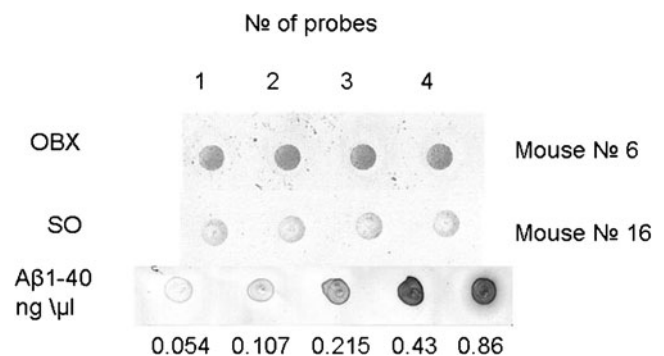

Fig. 2 The levels of pyknomorphic cells in various brain structures in different brain structures of SO and OBE mice 1.5 month after the surgery. *Cortex* temporal cortex, *Hipp* hippocampus, *NRD* nucleus raphe dorsalis, *NLC* nucleus locus coeruleus

Fig. 3 The levels of Aβ in OBX and SO mice as revealed by DOT blot analysis. The *two upper rows* depict representative dot blots from an OBX mouse and SO mouse correspondingly. Four samples (*dots*) were taken from each mouse for the analysis. The *bottom row* represents the calibration of the Aβ quantity
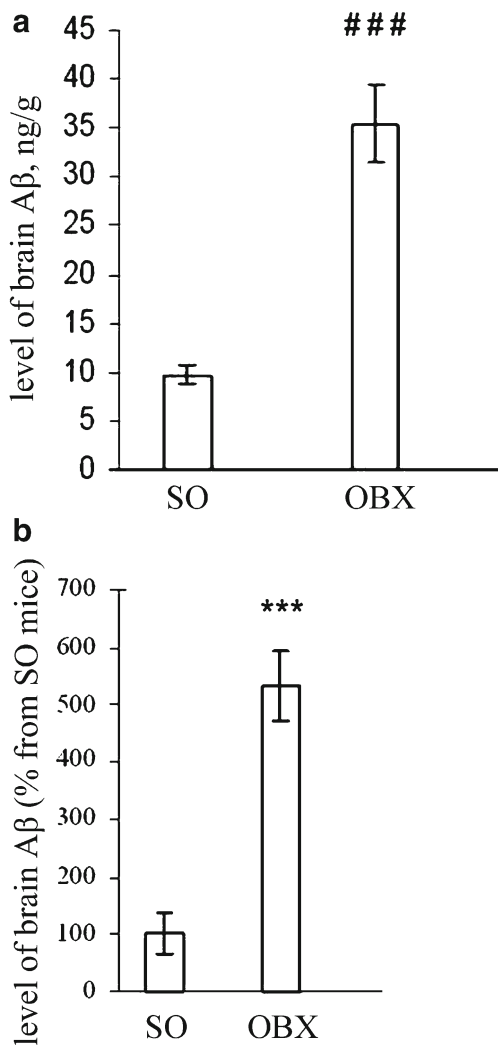
Fig. 4 Aβ accumulation in the brain of SO and OBX mice. *Bars* indicate the level of Aβ peptides (mean ± SEM) in the indicated groups of experimental mice (*n*=6–11 per group). **a** Aβ was determined by DOT analysis or **b** ELISA (see "Materials and methods"). The *bottom panel* shows the level of Aβ peptides in OBX group as values (mean ± SEM) relative to the content in SO group. The absolute value of Aβ in SO animals was 0.45 pM/g in the brain tissue (cortex + hippocampus). Differences between the levels of Aβ in the groups were determined by using the two-tailed Student's *t* test

The high level of endogenous Hsp70 in the brain coincides in time with amelioration of pathological consequences of the bulbectomy

The behavioral studies were carried out at 0.5, 1, 1.5, 3, 6, 8, 12, and 16 months after bulbectomy (eight groups of OBX and eight groups of SO animals, *n*=7–12 animals per group). Control sets of experiments conducted prior to the main training trials demonstrated that mean latencies for SO and OBX mice to reach the visible platform were approximately equal (data not shown). It indicates that bulbectomy per se did not induce motor or visual impairments that could

affect the results of the learning or memory test in Morris water maze. The comparison of latent periods to reach invisible platform in OBX and SO groups did show high significant effect of training days in all experimental periods tested. It means that all groups improved their performance (i.e., decreased time spent to reach invisible platform) with increased training. One-way ANOVA and post-hoc analysis using LSD criteria revealed no statistical difference in the learning abilities between SO and OBX groups over the 5-day training in all periods after removal of olfactory bulbs. At 24 h after the last training trial, mice were examined in a probe trial, when saving platform was removed from the water maze. Differences in probe trial parameters were evaluated with one-way ANOVA. A group analysis of variance was performed to evaluate the differences in occupancy time in each sector for each group and each period after the operation. Table 2 represents factor and post-hoc analysis of time spent by OBX and SO animals in sectors of Morris water maze in probe trials in different periods after bulbectomy. The data presented in Table 2 clearly show the recovery of spatial memory in OBX mice observed within 3 to 6 months after the surgery.

Figure 6a depicts the average time spent by OBX mice in the target sector of Morris water maze where rescue platform was located during probe trials. Since the experiments took almost 1 year which comprises a significant period in the mice life span, we should have taken into account a possible influence of aging on memory. Therefore, the data estimated for OBX animals were represented as percent from analogous characteristics established for SO mice from the same age group. Results of a Morris water maze test demonstrate a distinctive biphasic dynamic of spatial memory in OBX animals. By the end of the first month after bulbectomy, the OBX mice exhibited significant memory loss (Fig. 6a), which was almost completely restored by the sixth month postoperation. However, starting from the eighth month after the operation and extending to the end time point (16 months), OBX animals displayed a second, more profound deterioration of memory (Fig. 6a and Table 2).

In parallel, we measured an endogenous inducible form of Hsp70 by ELISA using specific antibodies in the brains of the mice after completion of the behavior analysis in 0.5, 3, 6, and 12 months after the surgery (Fig. 6b). Concomitant determination of endogenous Hsp70 level using specific antibodies has been performed in various brain regions. We failed to detect drastic changes in Hsp70 concentration in the temporal region and the entorhinal cortex in different postoperation periods mostly due to high variability in this character observed in OBX mice (data not shown). Basing on these observations, we presented the dynamics of Hsp70 changes in the hippocampus of OBX mice as a ratio of Hsp70 level of OBX animals to that of SO mice of the same age group in percent (Fig. 6b).
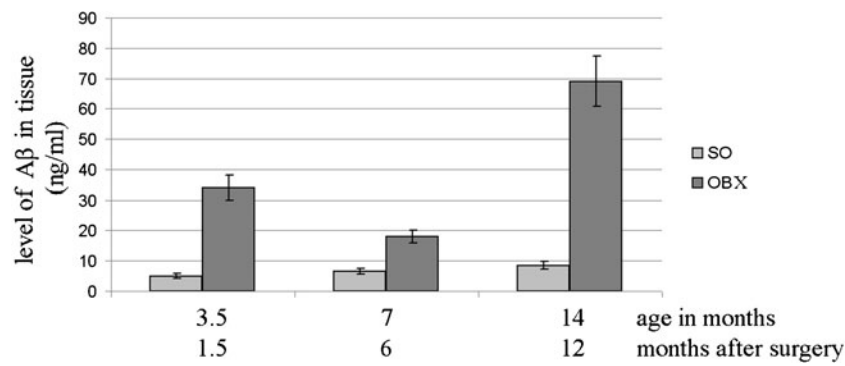
Fig. 5 Age-dependent fluctuations in Aβ levels in hippocampus of SO and OBX mice. *Bars* indicate the level of Aβ peptides (mean ± SEM) in the groups of experimental mice ($n=6–11$ per group). Aβ was determined by DOT analysis (see "Materials and methods").

Differences between the levels of Aβ were determined by using the two-tailed Student's t test in the SO and OBX groups at different age and time intervals after the surgery

Collectively, our studies demonstrate that there is a characteristic dynamics of Hsp70 level fluctuations in the hippocampus of OBX animals with a maximal peak in concentration observed approximately 6 months after bulbectomy (Fig. 6b). The comparison of data summarized in Fig. 6a and b demonstrates clear-cut time coincidence between almost complete recovery of spatial memory in OBX mice with the maximal peak in the inducible Hsp70 level in the hippocampus, a brain region playing the pivotal role in memory and learning.

Discussion

Epidemiological studies support the hypothesis that TBI is one of the major risk factors for AD (Van den Heuvel et al. 2007). However, it is unknown how exactly TBI or other brain injuries may trigger the neurodegenerative cascade leading to AD. Since usually a significant time gap is observed between the TBI and the development of secondary consequences similar to AD symptoms, it is possible that activation of certain innate compensatory mechanisms

Table 2 Dynamic of memory changes in different time periods after bulbectomy (ANOVA analysis of occupancy time in sectors of water maze in OBX and SO mice in different periods after bulbectomy)

Period after bulbectomy (months)	Groups of mice	F	P	Time spent by mice in different sectors			
				Indifferent sector 1	Indifferent sector 2	Target sector 3	Indifferent sector 4
0.5	Probe trial	SO ($n=12$)	37.75	0.000***	14.0±0.43***	10.46±1.31***	25.77±1.66	9.0±1.08***
		OBE ($n=9$)	14.43	0.0001***	13.77±0.99***	11.77±1.02***	22.31±1.74	12.15±1.52***
1	Probe trial	SO ($n=12$)	13.52	0.000***	9.75±1.85***	7.75±1.26***	32.0±1.99	13.2±2.06***
		OBE ($n=9$)	2.65	0.066	12.0±1.45	13.0±1.56	17.0±1.59	14.11±2.14
1.5	Probe trial	SO ($n=10$)	26.79	0.000***	10.7±1.76***	9.4±1.05***	28.4±2.57	11.0±1.42***
		OBE ($n=7$)	0.798	0.515	16.0±1.45	12.8±2.27	13.4±3.75	17.8±3.54
3	Probe trial	SO ($n=12$)	99.46	0.000***	11.5±1.1***	10.5±1.14***	27.3±2.08	10.75±0.73***
		OBE ($n=7$)	4.69	0.001**	18.14±1.68	7.57±2.11**	22.57±3.25	11.71±2.24**
6	Probe trial	SO ($n=12$)	12.04	0.000***	14.42±1.06**	11.25±0.9***	23.42±1.95	11.33±1.33***
		OBE ($n=7$)	4.44	0.013*	12.86±2.73*	13.29±2.33*	24.43±0.94	15.29±1.71*
8	Probe trial	SO ($n=9$)	13.92	0.000***	10.78±1.73***	15.11±2.06**	26.44±2.29	8.89±1.38***
		OBE ($n=9$)	4.53	0.009**	16.22±1.63	15.22±1.76	18.11±1.67	10.44±1.43*
12	Probe trial	SO ($n=9$)	40.89	0.000***	10.33±1.59***	9.67±0.57***	29.0±2.06	12.11±1.41***
		OBE ($n=12$)	4.9	0.0051**	17.92±2.03	10.33±0.91*	17.89±1.92	13.17±2.69
16	Probe trial	SO ($n=9$)	6.86	0.001**	10.8±1.8***	14.61±1.5**	22.43±1.8	12.22±1.62**
		OBE ($n=9$)	1.06	0.398	15.0±1.24	14.1±1.21	13.48±1.32	16.5±1.32

Significance of differences between target (3rd sector) and other indifferent sectors
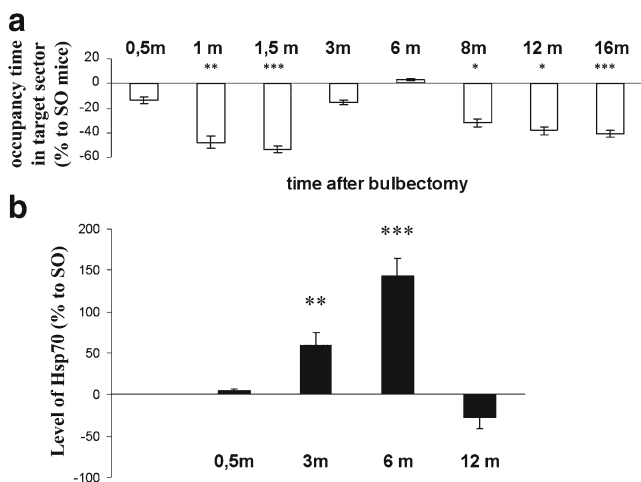
* $p<0.05$; ** $p<0.01$; *** $p<0.001$

Fig. 6 Maximal endogenous Hsp70 level coincides in time with spatial memory recovery in OBX mice. The level of spatial memory (**a**) strongly correlates with the hippocampal concentration of endogenous Hsp70 (**b**) in OBX mice. *Top panel* (**a**) shows the values (mean ± SEM) of the ratios between times spent by animals of OBX and control sham-operated (SO) groups ($n=7$–13 per group) in a target sector of a Morris water maze during probe trails. Values are expressed as a function of time (months postoperation period). After completion of the behavioral experiments, animals from each age group were euthanized and their brains were used for Hsp70 measurements. The bottom panel (**b**) shows the values (mean ± SEM) representing the ratio of Hsp70 concentrations between OBX and SO animals at 0.5; 3; and 6 and 12 months after OBX. The absolute values (ng/g) of Hsp70 in SO animals after 0.5, 3, 6, and 12 months were 6.2±2.1, 7.8±1.4, 5.2±0.9, and 12.95±3.5, respectively

may ameliorate for some time the harmful consequences of brain damage, thereby precluding neuronal death. On the other hand, abundant data exist on the protective role of endogenous Hsps in various neurodegenerative diseases and aging (Calderwood et al. 2009; Merlin and Sherman 2005; Sheng and Brown 2007; Gifondorwa et al. 2007; Magrané et al. 2004; Magrane and Querfurth 2010).

A large body of data, including our own results, indicates that injury of the olfactory bulbs in rodents sets off many symptoms similar to major manifestations of AD (Bobkova et al. 2005; Doty 2009; Skelin et al. 2008). Importantly, it was shown using several transgenic animal models of AD that accumulation of amyloid-β starts in the glomerular layer of the olfactory bulbs (Wesson et al. 2010). The high level of survival in animals after bulbectomy as well as massive neuronal loss due to axon degeneration coupled with a sharp increase of amyloid precursor protein and Aβ (Struble et al. 1998; Bobkova et al. 2008; Kaminina et al. 2010) make OBX mice a model of choice to study TBI-triggered neurodegeneration.

Our experiments described herein revealed biphasic dynamics of spatial memory deterioration in OBX animals with almost complete recovery observed within 4–6 months interval after the operation (Fig. 6 and Table 2). Interestingly, in OBE group, the minimal level of Aβ was

observed in 5–7 months after the operation (Fig. 5). We speculated that activation of certain protective innate mechanisms may be responsible for the provisional amelioration of the harmful consequences of brain damage.

Here we describe a clear-cut coincidence in time between the state of spatial memory, amyloid-β levels, and endogenous Hsp70 content in the hippocampus of OBX animals (Figs. 5 and 6). These data enabled us to suggest that Hsp70 induction after olfactory bulb ablation is somehow involved in activation of compensatory mechanisms averting the development of neurodegeneration after brain injury in OBX mice. It was shown along these lines that in the nervous system, as in other tissues, the induction of Hsps not only serves as marker for stress but has a significant protective effect as well (Tidwell et al. 2004; Sheng and Brown 2007).

The protective effect of endogenous Hsp70 can be due not only to the direct chaperone activity against high level of misfolded Aβ in the brains of OBX mice. It is also possible that Hsp70 induction may stimulate other systems that are responsible for cell survival after brain injury (Seidberg et al. 2003; Robinson et al. 2005). Cumulative indirect effects of Hsp70, such as suppression of apoptosis (Tidwell et al. 2004), lysosome stabilization (Kirkegaard et al. 2010), stimulation of the innate immune response (Johnson and Fleshner 2006; Gong et al. 2009), suppression of the early preoligomeric stages of Aβ self-assembly (Evans et al. 2006; Calderwood 2010), inhibition of proinflammatory signaling (Rozhkova et al. 2010), and increase of survival of endogenous neural progenitor cells (Doeppner et al. 2009) may account for the observed correlation. Possibly, Hsp70 induction somehow activates other compensatory mechanisms that facilitate regeneration and help to restore for some time normal functioning of neurons after the injury. Further studies need to be undertaken in order to understand the mechanisms by which Hsp70 most likely regulates various neurodegenerative disease pathologies.

If the protective paradigm of endogenous Hsp70 induction is widespread, various drugs enhancing its synthesis or direct administration of this chaperone into the brain may represent a conceptually novel model for the practical treatment of some of the most common neurodegenerative conditions, including AD, Parkinson's, ALS, and other neurodegenerative diseases, for which no effective treatment currently exists. Taken together, our findings suggest possible neuroprotective functions of endogenous Hsp70 and establish this chaperone as a promising pharmacological agent to prevent consequences of brain injury often accompanied by profound neuronal death and cognitive disturbances.

References

Bobkova NV, Nesterova IV, Medvinskaya NI, Aleksandrova IY, Samokhin AN, Gershovich YG, Gershovich PM, Yashin VA (2005) Possible role of olfactory system in Alzheimer's disease genesis. In: Hanin L, Fisher A, and Monduzzi M (eds) Alzheimer's and Parkinson's disease—AD/PD pp 91–95

Bobkova N, Vorobyov V, Medvinskaya N, Aleksandrova I, Nesterova I (2008) Interhemispheric EEG differences in olfactory bulbectomized rats with different cognitive abilities and brain beta-amyloid levels. Brain Res 1232:185–194

Calderwood SK (2010) Protein quality control and heat shock gene expression in the nervous system. In: Asea A, Calderwood SK (eds) Heat shock proteins and the brain: implications for neurodegenerative diseases and neuroprotection. Springer

Calderwood SK, Murshid A, Prince T (2009) The shock of aging: molecular chaperones and the heat shock response in longevity and aging—a mini-review. Gerontology 55:550–558

Chételat G, Landeau B, Eustache F, Mézenge F, Viader F, de la Sayette V, Desgranges B, Baron JC (2005) Using voxel-based morphometry to map the structural changes associated with rapid conversion in MCI: a longitudinal MRI study. NeuroImage 27:934–946

Cummings CJ, Sun Y, Opal P, Antalffy B, Mestril R, Orr HT, Dillmann WH, Zoghbi HY (2001) Over-expression of inducible HSP70 chaperone suppresses neuropathology and improves motor function in SCA1 mice. Hum Mol Genet 10:1511–1518

Doeppner TR, Nagel F, Dietz GP, Weise J, Tönges L, Schwarting S, Bähr M (2009) TAT-Hsp70-mediated neuroprotection and increased survival of neuronal precursor cells after focal cerebral ischemia in mice. J Cereb Blood Flow Met 29:1187–1196

Doty RL (2009) The olfactory system and its disorders. Semin Neurol 29:74–81

Evans CG, Wisén S, Gestwicki JE (2006) Heat shock proteins 70 and 90 inhibit early stages of amyloid beta-(1–42) aggregation in vitro. J Biol Chem 281:33182–33191

Franklin TB, Krueger-Naug AM, Clarke DB, Arrigo AP, Currie RW (2005) The role of heat shock proteins Hsp70 and Hsp27 in cellular protection of the central nervous system. Int J Hyperthermia 21:379–392

Gifondorwa DJ, Robinson MB, Hayes CD, Taylor AR, Prevette DM, Oppenheim RW, Caress J, Milligan CE (2007) Exogenous delivery of heat shock protein70 increases lifespan in a mouse model of amyotrophic lateral sclerosis. J Neurosci 27:13173–13180

Gong J, Zhu B, Murshid A, Adachi H, Song B, Lee A, Liu C, Calderwood SK (2009) T cell activation by heat shock protein 70 vaccine requires TLR signaling and scavenger receptor expressed by endothelial cells-1. J Immunol 183:3092–3098

Hemphill JC, Andrews P, De Georgia M (2011) Medscape. Multimodal monitoring and neurocritical care bioinformatics. Nat Rev Neurol 7:451–460

Holland D, Brewer JB, Hagler DJ, Fennema-Notestine C, Dale AM, Alzheimer's disease neuroimaging initiative (2009) Subregional neuroanatomical change as a biomarker for Alzheimer's disease. Proc Natl Acad Sci USA 106:20954–20959

Hoshino T, Murao N, Namba T, Takehara M, Adachi H, Katsuno M, Sobue G, Matsushima T, Suzuki T, Mizushima T (2011) Suppression of Alzheimer's disease-related phenotypes by expression of heat shock protein 70 in mice. J Neurosci 31:5225–5234

Hozumi S, Nakagawasai O, Tan-No K, Niijima F, Yamadera F, Murata A, Arai Y, Yasuhara H, Tadano T (2003) Characteristics of changes in cholinergic function and impairment of learning and memory-related behavior induced by olfactory bulbectomy. Behav Brain Res 138:9–15

Ikonomovic MD, Uryu K, Abrahamson EE, Ciallella JR, Trojanowski JQ, Lee VM, Clark RS, Marion DW, Wisniewski SR, DeKosky ST (2004) Alzheimer's pathology in human temporal cortex surgically excised after severe brain injury. Exp Neurol 190:192–203

Johnson JD, Fleshner M (2006) Releasing signals, secretory pathways, and immune function of endogenous extracellular heat shock protein 72. J Leukoc Biol 79:425–434

Johnson VE, Stewart W, Douglas HS (2010) Traumatic brain injury and amyloid-β pathology: a link to Alzheimer's disease? Nat Rev Neurosci 11:361–370

Kaminina AV, Volpina OM, Medvinskaya NI, Aleksandrova IJ, Volkova TD, Koroev DO, Samokhin AN, Nesterova IV, Shelukhina IV, Kryukova EV, Tsetlin VI, Ivanov VT, Bobkova NV (2010) Vaccination with peptide 173–193 of acetylcholine receptor alpha7-subunit prevents memory loss in olfactory bulbectomized mice. J Alzheimer Dis 21:249–261

Kirkegaard T, Roth AG, Petersen NH, Mahalka AK, Olsen OD, Moilanen I, Zylicz A, Knudsen J, Sandhoff K, Arenz C, Kinnunen PK, Nylandsted J, Jäättelä M (2010) Hsp70 stabilizes lysosomes and reverts Niemann–Pick disease-associated lysosomal pathology. Nature 463:549–553

Klapdor K, Van der Staay FJ (1996) The Morris water-escape task in mice: strain differences and effects of intra-maze contrast and brightness. Physiol Behav 60:1247–1254

Kustanova G, Murashev A, Karpov V, Margulis B, Guzhova IV, Prokhorenko IR, Grachev SV, Evgen'ev MB (2006) Exogenous heat shock protein 70 mediates sepsis manifestations and decreases the mortality rate in rats. Cell Stress Chaperones 11:276–286

Magrane J, Querfurth HW (2010) Heat shock proteins: unfolded protein response chaperones and Alzheimer's diseases.In: Asea AA, Brown IR (eds) Heat shock proteins and the brain: implications for neurodegenerative diseases and neuroprotection, Springer pp 25–50

Magrané J, Smith RC, Walsh K, Querfurth HW (2004) Heat shock protein 70 participates in the neuroprotective response to intracellularly expressed beta-amyloid in neurons. J Neurosci 24:1700–1706

Margulis B, Kinev A, Guzhova I (2006) In: Radons J, Multhoff G (eds) Heat shock proteins in biology and medicine, Research Singpost pp 305–330

Merlin AB, Sherman MY (2005) Role of molecular chaperones in neurodegenerative disorders. Int J Hyperthermia 21:403–419

Moriguchi S, Han F, Nakagawasai O, Tadano T, Fukunaga K (2006) Decreased calcium/calmodulin-dependent protein kinase II and protein kinase C activities mediate impairment of hippocampal long-term potentiation in the olfactory bulbectomized mice. J Neurochem 97:22–29

Nakajima A, Yamakuni T, Haraguchi M, Omae N, Song SY, Kato C, Nakagawasai O, Tadano T, Yokosuka A, Mimaki Y, Sashida Y, Ohizumi Y (2007) Nobiletin, a citrus flavonoid that improves memory impairment, rescues bulbectomy-induced cholinergic neurodegeneration in mice. J Pharmacol Sci 105:122–126

Nesterova IV, Gurevich EV, Nesterov VI, Otmakhova NA, Bobkova NV (1997) Bulbectomy-induced loss of raphe neurons is counteracted by antidepressant treatment. Prog Neuro-Psychopharm Biol Psychiatry 2:127–140

Nesterova IV, Bobkova NV, Medvinskaya NI, Samokhin AN, Aleksandrova IY (2008) Morphofunctional state of neurons in the temporal cortex and hippocampus in relation to the level of spatial memory in rats after ablation of the olfactory bulbs. Neurosc Behav Physiol 38:349–353

Reisberg B, Saeed MU (2004) In: Sadavoy, J. et al. (eds) Comprehensive textbook of geriatric psychiatry. Third Edition., Norton, New York. pp 449–509

Robinson MB, Tidwell JL, Gould T, Taylor AR, Newbern JM, Graves J, Tytell M, Milligan CE (2005) Extracellular heat shock protein 70: a critical component for motoneuron survival. J Neurosci 25:9735–9745

Rozhkova E, Yurinskaya M, Zatsepina O, Garbuz D, Karpov V, Surkov S, Murashev A, Ostrov V, Margulis B, Evgen'ev M, Vinokurov M (2010) Exogenous mammalian extracellular HSP70 reduces endotoxin manifestations at the cellular and organism levels. Ann N Y Acad Sci 1197:94–107

Seidberg NA, Clark RS, Zhang X, Lai Y, Chen M, Graham SH, Kochanek PM, Watkins SC, Marion DW (2003) Alterations in inducible 72-kDa heat shock protein and the chaperone cofactor BAG-1 in human brain after head injury. J Neurochem 84:514–521

Sheng C, Brown IR (2007) Neuronal expression of constitutive heat shock proteins: implications for neurodegenerative diseases. Cell Stress Chaperones 12(1):51–58

Skelin I, Sato H, Diksic M (2008) Olfactory bulbectomy reduces cerebral glucose utilization: 2-[14C] deoxyglucose autoradiographic study. Brain Res Bull 76:485–492

Song C, Leonard BE (2005) The olfactory bulbectomised rat as a model of depression. Neurosci Biobehav Rev 29:627–647

Struble RG, Dhanraj DN, Mei Y, Wilson M, Wang R, Ramkumar V (1998) Beta-amyloid precursor protein-like immunoreactivity is upregulated during olfactory nerve regeneration in adult rats. Brain Res 780:129–137

Tidwell JL, Houenou LJ, Tytell M (2004) Administration of Hsp70 in vivo inhibits motor and sensory neuron degeneration. Cell Stress Chaperones 9:88–98

Toyn JH, Lin XA, Thompson MW, Guss V, Meredith JE Jr, Sankaranarayanan S, Barrezueta N, Corradi J, Majumdar A, Small DL, Hansard M, Lanthorn T, Westphal RS, Albright CF (2010) Viable mouse gene ablations that robustly alter brain Abeta levels are rare. BCM Neuroscience 11:143–151

Van den Heuvel C, Thornton E, Vink R (2007) Traumatic brain injury and Alzheimer's disease: a review. Prog Brain Res 161:303–316

Wacker JL, Huang SY, Steele AD, Aron R, Lotz GP, Nguyen Q, Giorgini F, Roberson ED, Lindquist S, Masliah E, Muchowski PJ (2009) Loss of Hsp70 exacerbates pathogenesis but not levels of fibrillar aggregates in a mouse model of Huntington's disease. J Neurosci 29:9104–9114

Wang HC, Ma YB (2010) Experimental models of traumatic axonal injury. J Clin Neurosci 17:157–162

Wesson DW, Levy E, Nixon RA, Wilson DA (2010) Olfactory dysfunction correlates with amyloid-beta burden in an Alzheimer's disease mouse model. J Neurosci 30:505–514